Electron-Phonon Interaction in NbB_2 : A Comparison with MgB_2

Prabhakar P. Singh

Department of Physics, Indian Institute of Technology, Powai, Mumbai- 400076, India

Abstract

We present a comparison of electron-phonon interaction in NbB_2 and MgB_2, calculated using full-potential, density-functional-based methods in $P6/mmm$ crystal structure. Our results, described in terms of (i) electronic structure, (ii) phonon density of states $F(\omega)$, (iii) Eliashberg function $\alpha^2F(\omega)$, and (iv) the solutions of the isotropic Eliashberg gap equation, clearly show significant differences in the electron-phonon interaction in NbB_2 and MgB_2. We find that the average electron-phonon coupling constant λ is equal to 0.59 for MgB_2 and 0.43 for NbB_2, leading to superconducting transition temperature T_c of around $22\,K$ for MgB_2 and $3\,K$ for NbB_2.

The lack of success in finding superconductivity in other diborides with superconducting transition temperature, T_c, close to that of MgB_2 [1] underscores the complex nature of interaction responsible for superconductivity in MgB_2. In MgB_2 the complexity is further compounded by the presence of multi-faceted Fermi surface [2,3] and a highly anisotropic electron-phonon coupling, $\lambda(\mathbf{k},\mathbf{k}')$, over the Fermi surface [4,5]. The dependence of superconducting properties on such details has ensured that we do not know, as yet, the exact nature of interaction leading to superconductivity in MgB_2.

Within Eliashberg-Migdal theory [6,7] of superconductivity, a reliable description of the superconducting state requires an accurate knowledge of $\lambda(\mathbf{k},\mathbf{k}')$ and the renormalized electron-electron interaction, μ^*, which are used as input to the fully anisotropic gap equation. The present computational capability allows us to evaluate $\lambda(\mathbf{k},\mathbf{k}')$ accurately using density-functional-based methods but, unfortunately, μ^* cannot be evaluated. However, it is reasonable to assume that μ^* varies between 0.1 to 0.2 [4,5]. Thus, the electron-phonon coupling $\lambda(\mathbf{k},\mathbf{k}')$, which is a normal state function, must contain signatures of superconducting state.

In an attempt to identify some of the unique features of electron-phonon interaction in MgB_2 *vis-a-vis* other diborides we have studied (i) the electronic structure, (ii) the phonon density of states (DOS), (iii) the Eliashbrg function, and (iv) the solutions of the isotropic Eliashberg gap equation for NbB_2 and MgB_2 in $P6/mmm$ crystal structure.

The choice of NbB_2 has been motivated by the recent reports [8,9] of superconductivity, with T_c going up to $9.2\,K$, under pressure in hole-doped Nb_xB_2. Earlier experiments have shown superconductivity in stoichiometric NbB_2 [9,10] as well as Boron-enriched NbB_2 [11] samples. The reported T_c for stoichiometric NbB_2 varies from $0.62\,K$ [10] to $5.2\,K$ [9], while for Boron-enriched $NbB_{2.5}$ the T_c is found to be $6.4\,K$ [11]. We also note that, recently, Kaczorowski *et al.* [12] did not find any superconductivity in NbB_2 down to $2\,K$.

We have calculated the electronic structure of NbB_2 and MgB_2 in $P6/mmm$ crystal structure with optimized lattice constants a and c, as given in Table I. The lattice constants a and c were optimized using the ABINIT program [13] based on pseudopotentials and plane waves. For studying the electron-phonon interaction we used the full-potential linear response program of Savrasov [14,15], and calculated the dynamical matrices and the Hopfield parameter. These were then used to calculate the phonon DOS, $F(\omega)$, the electron-phonon coupling $\lambda(\mathbf{k},\mathbf{k}')$, and the Eliashberg function, $\alpha^2F(\omega)$, for NbB_2 and MgB_2. Subsequently, we have numerically solved the isotropic Eliashberg gap equation [6,7,16] for a range of μ^* to obtain the corresponding T_c.

Based on our calculations, described below, we find significant differences in the phonon DOS and the Eliashberg functions of NbB_2 and MgB_2. In particular, we find that the average electron-phonon coupling constant is equal to 0.59 for MgB_2 and 0.43 for NbB_2, leading to superconducting transition temperatures of around $22\,K$ for MgB_2 and $3\,K$ for NbB_2.

Before describing our results in detail, we provide some of the computational details of our calculation. The structural relaxation was carried out by the molecular dynamics program ABINIT [13] with Broyden-Fletcher-Goldfarb-Shanno minimization technique using Troullier-Martins pseudopotential [18] for MgB_2 and Hartwigsen-Goedecker-Hutter pseudopotential [19] for NbB_2, 512 Monkhorst-Pack [20] k-points and Teter parameterization for exchange-correlation. The kinetic energy cutoff for the plane waves was $110\,Ry$ for MgB_2 and $140\,Ry$ for NbB_2. The charge self-consistent full-potential LMTO [14] calculations were carried out with the generalized gradient approximation for exchange-correlation of Perdew *et al* [21] and 484 k-points in the irreducible wedge of the Brillouin zone. For MgB_2, the basis set used consisted of 3κ panels and s, p, d and f orbitals at the Mg site and s, p and d orbitals at the B site. In the case of NbB_2, we included 2κ panels and s, p and d orbitals at the Nb site. In all cases the potential and the wave function were expanded

Table 1
The calculated lattice constants a and c. The experimental lattice constants for MgB_2 [17] and NbB_2 are shown in the parentheses.

	a (a.u.)	c (a.u.)
MgB_2	5.76 (5.834)	6.59 (6.657)
NbB_2	5.81 (5.837)	6.10 (6.245)

Table 2
The site- and l-resolved electronic densities of states, in $st/(Ry-atom)$, at the Fermi energy in MgB_2 and NbB_2 calculated at the optimized lattice constants using the full-potential LMTO method.

alloy	element	s	p	d	f
MgB_2	Mg	0.47	0.72	0.94	0.08
	B	0.06	3.36	0.15	-
NbB_2	Nb	0.02	.09	9.54	-
	B	0.07	1.34	0.19	-

up to $l_{max} = 6$. The muffin-tin radii for Mg, B, and Nb were taken to be 2.4, 1.66, and 2.3 atomic units, respectively.

The calculation of dynamical matrices and the Hopfield parameters for MgB_2 were carried out using a $6 \times 6 \times 6$ grid while for NbB_2 we used a $4 \times 4 \times 4$ grid resulting in 28 and 12 irreducible **q**-points, respectively. For Brillouin zone integrations in MgB_2 we used a $6 \times 6 \times 6$ grid while for NbB_2 we used $8 \times 8 \times 8$ grid of **k**-points. The Fermi surface was sampled more accurately with a $24 \times 24 \times 24$ grid of **k**-points using the double grid technique as outlined in Ref. [15].

Here, we like to point out the reasons for carrying out the linear response calculation for MgB_2 in spite of earlier calculations by Kong *et al.* [4] and Choi *et al.* [3,5]. The linear response calculation by Kong *et al.* is similar to the present approach, while Choi *et al.* used pseudopotentials and frozen phonon method to evaluate the electron-phonon coupling $\lambda(\mathbf{k}, \mathbf{k}')$. The present approach differs from the work of Kong *et al* in the selection of **q**-points and the Brillouin zone integrations. As a result Kong *et al.* find the average electron-phonon coupling constant $\lambda = 0.87 \pm 0.05$, which is much higher than the value of $\lambda = 0.61$ as reported by Choi *et al.* [3,5], as well as the experimental values of 0.58 [22] and 0.62 [23] as deduced from specific heat measurements. Our calculated value of λ is equal to 0.59, in close agreement with the work of Choi *et al.*.

A comparison of site- and l-resolved electronic density of states of NbB_2 [24] and MgB_2 [25] at the Fermi energy is given in Table II. A further

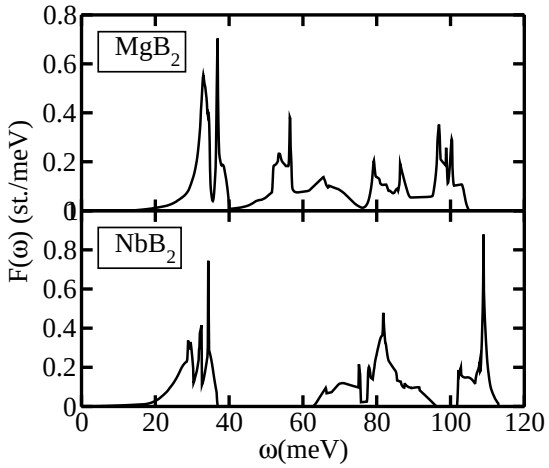

Fig. 1. The phonon density of states $F(\omega)$ of MgB_2 and NbB_2 calculated using the full-potential linear response method as described in the text.

decomposition of the densities of states (st/Ry) in terms of cubic harmonics reveals the dominance of B p electrons at the Fermi energy in MgB_2 ($p_{x(y)} = 0.9$, $p_z = 1.55$) than in NbB_2 ($p_{x(y)} = 0.43$, $p_z = 0.48$). In addition, in NbB_2, the Nb d-electrons ($d_{xy(x^2-y^2)} = 1.83$, $d_{yz(zx)} = 1.66$, $d_{3z^2-1} = 2.56$) are present in substantial amount, indicating a more active role for Nb in determining the possible superconducting properties of these materials than played by Mg in MgB_2.

In Fig. 1 we show the phonon DOS $F(\omega)$ of NbB_2 and MgB_2 calculated using the full-potential linear response program as described earlier. For MgB_2 we can clearly identify four significant peaks in the phonon DOS at 33, 53, 79 and 96 meV, respectively. The peak at 33 meV is related to the van Hove singularity in the acoustical mode [5], and it involves the motion of Mg atom and B atoms separately. However, the region around the peak at 53 meV results from the motion of both Mg and B atoms. The phonon DOS around 79 and 96 meV peaks are due to the coupled motion of $B-B$ atoms in the $x-y$ plane. In particular, the peak at 79 meV corresponds to the in-plane $B-B$ bond stretching mode, and in Ref. [5] it is located at $77\,meV$. Similarly, for NbB_2, the peak in $F(\omega)$ at 32 meV is dominated by the motion of Nb atom, while the region around $65-70$ meV results from the coupled motion of Nb and the two B atoms. Not surprisingly, 81 meV peak in the phonon DOS of NbB_2 corresponds to the in-plane $B-B$ motion. In contrast with the phonon DOS in MgB_2, the phonon DOS in NbB_2 around 106 meV results from the displacements of both Nb and the two B atoms.

To see the strengths with which the different modes of the ionic motion couple to the electrons, and thus are capable of influencing the superconducting prop-

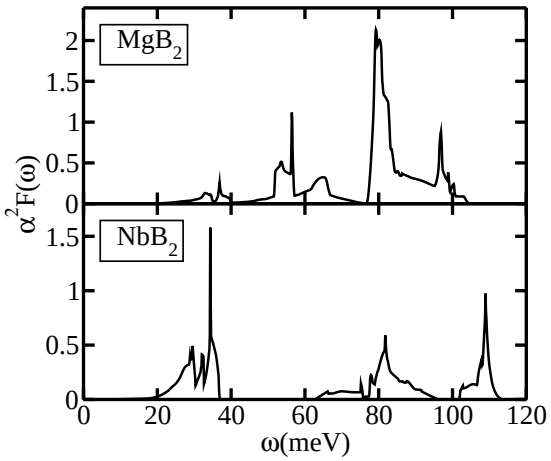

Fig. 2. The Eliashberg function $\alpha^2F(\omega)$ of MgB_2 and NbB_2 calculated using the full-potential linear response method as described in the text.

erties the most, we show in Fig. 2 the Eliashberg function $\alpha^2F(\omega)$ of NbB_2 and MgB_2 calculated as described earlier. The most striking feature of Fig. 2 is the overall strength of the electron-phonon coupling in MgB_2 as compared to NbB_2. We find that the average electron-phonon coupling constant λ is equal to 0.59 for MgB_2 and 0.43 for NbB_2, which clearly shows that MgB_2 is more likely to show superconductivity with a higher T_c than NbB_2.

Further analysis of the Eliashberg function, as shown in Fig. 2, reveals the importance of the in-plane $B-B$ bond-stretching optical phonon mode in MgB_2, which gives rise to the dominant peak at $79\,meV$. The other peaks in the phonon DOS of MgB_2, such as the peaks at 33 and 53 meV, couple weakly with the electrons at the Fermi energy. Thus the motion of Mg atom plays a relatively insignificant role in determining the superconducting properties of MgB_2. In contrast, in the case of NbB_2 the phonon modes with peaks at 32, 81 and 106 meV couple to the electrons with almost equal strength, albeit much smaller than in MgB_2, as can be seen from Fig. 2. We could have expected this because of the significant presence of the Nb d electrons at the Fermi energy. In Table III we have listed the Hopfield parameter η, the electron-phonon coupling constant λ, and the various averages of the phonon frequencies for NbB_2 and MgB_2. The values listed in Table III for MgB_2 are in good agreement with the corresponding results of Choi *et al.* [5].

To examine the superconducting transition temperature, *if* any, of NbB_2 and MgB_2 we have used the calculated Eliashberg function $\alpha^2F(\omega)$ to solve numerically the isotropic gap equation [7,16], and the results are shown in Fig. 3 for a range of values of μ^*. From Fig. 3 we find that for $\mu^* = 0.1$ the T_c for MgB_2 is equal to $\sim 23\,K$, while for NbB_2 it is equal to $\sim 4\,K$. Thus, our

Table 3
The calculated Hopfield parameter η, the average electron-phonon coupling constant λ, the root mean square $< \omega^2 >^{1/2}$ and the logarithmically averaged ω_{ln} phonon frequencies for MgB_2 and NbB_2.

alloy	$\eta\,(mRy/a.u.^2)$	λ	$< \omega^2 >^{1/2}\ (K)$	$\omega_{ln}\,(K)$
MgB_2	167	0.59	835	768
NbB_2	203	0.43	669	494

calculation shows that NbB_2 is superconducting with a possible T_c of around $3\,K$. It is worthwhile to point out that to obtain a T_c close to that of $39\,K$ for MgB_2, as found experimentally [1], one has to solve the *anisotropic* gap equation [5]. The need to solve the anisotropic gap equation for MgB_2 rather than the isotropic gap equation arises due to the highly anisotropic electron-phonon coupling $\lambda(\mathbf{k}, \mathbf{k}')$ [3–5] over the Fermi surface. In the case of NbB_2 the electron-phonon coupling is *neither as strong nor as anisotropic*, and thus the results obtained with the isotropic gap equation are reliable.

As indicated earlier, the experiments show superconductivity in hole-doped Nb_xB_2 under pressure and Boron-enriched NbB_2. Hole-doping and Boron enriching both lead to a relative increase in the Boron population at the Fermi energy and, probably, enhances the peak around $81\,meV$ leading to an increase in T_c. Of course a more quantitative investigation is needed to pinpoint the exact nature of changes in NbB_2 which lead to superconductivity.

In conclusion, we have studied the electron-phonon interaction in NbB_2 and MgB_2, using full-potential, density-functional-based methods in $P6/mmm$ crystal structure. We have described our results in terms of (i) electronic structure, (ii) phonon density of states, (iii) Eliashberg function, and (iv) the solutions of the isotropic Eliashberg gap equation, which clearly show significant differences in the electron-phonon interaction in NbB_2 and MgB_2. We find that the average electron-phonon coupling constant is equal to 0.59 for MgB_2 and 0.43 for NbB_2, leading to superconducting transition temperature of around $22\,K$ for MgB_2 and $3\,K$ for NbB_2.

References

[1] J. Akimitsu, Symp. on Transition Metal Oxides, Sendai, January 10, 2001; J. Nagamatsu, *et al.*, Nature **410**, 63 (2001).

[2] Kortus e*t al.*, Phys. Rev. Lett. **86**, 4656 (2001).

[3] Choi *et al.*, cond-mat/0111183.

[4] Kong *et al.*, Phys. Rev. B **64** 20501 (2001).

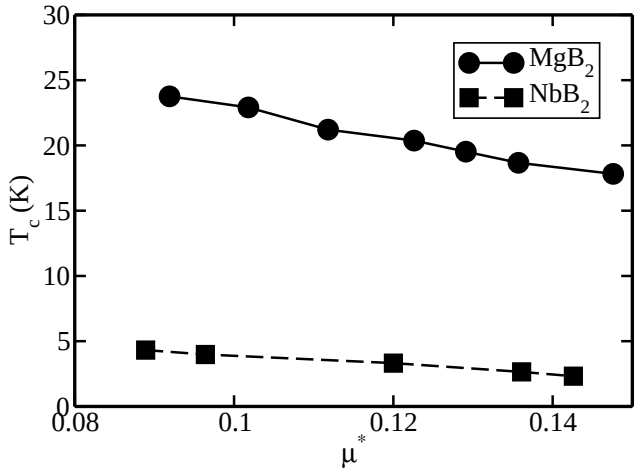

Fig. 3. The superconducting transition temperature T_c as a function of μ^* for MgB_2 and NbB_2 as obtained from the isotropic Eliashberg gap equation.

[5] Choi *et al.*, cond-mat/0111182.

[6] P. B. Allen and B. Mitrovic, in Solid State Physics, edited by H. Ehrenreich, F. Seitz, D. Turnbull (Academic, New York 1982), Vol. **37**, p.1. and references therein.

[7] P. B. Allen and R. C. Dynes, Phys. Rev. B **12**, 905 (1975).

[8] Yamamoto *et al.*, cond-mat/0208331.

[9] Akimitsu *et al.*, as cited in Ref. [8].

[10] L. Layarovska and E. Layarovski, J. Less Common Met. **67**, 249 (1979).

[11] Cooper *et al.*, Proc. Nat. Acad. Sci. **67**, 313 (1970).

[12] D. Kaczorowski *et al.*, cond-mat/0103571.

[13] http://www.abinit.org/.

[14] S. Y. Savrasov, Phys. Rev. B 54, 16470 (1996).

[15] S. Y. Savrasov and D. Y. Savrasov, Phys. Rev. B 54, 16487(1996).

[16] P. B. Allen, private communication.

[17] A. Lipp and M. Roder, Z. Anorg. Allg. Chem. **344**, 225 (1966).

[18] N. Troullier and J. L. Martins, Phys. Rev. B **43**, 1993 (1991).

[19] Hartwigsen *et al.*, Phys. Rev. B **58**, 3641 (1998).

[20] H. J. Monkhorst and J. D. Pack, Phys. Rev. B **13**, 5188 (1976).

[21] J. P. Perdew and Y. Wang, Phys. Rev. B **45**, 13244 (1992); J. Perdew *et al.*, Phys. Rev. Lett. **77**, 3865 (1996).

[22] Wang *et al.*, Physica C **355**, 179 (2001).

[23] Bouquet *et al.*, Phys. Rev. Lett. **87**, 47001 (2001).

[24] Prabhakar P. Singh, unpublished.

[25] Prabhakar P. Singh, Phys. Rev. Lett. **87**, 87004 (2001).